Spin Noise Spectroscopy in Rb Vapor

Nicholas Krueger & Paul Crowell
School of Physics and Astronomy
University of Minnesota Twin Cities
Minneapolis, Minnesota

Apparatus

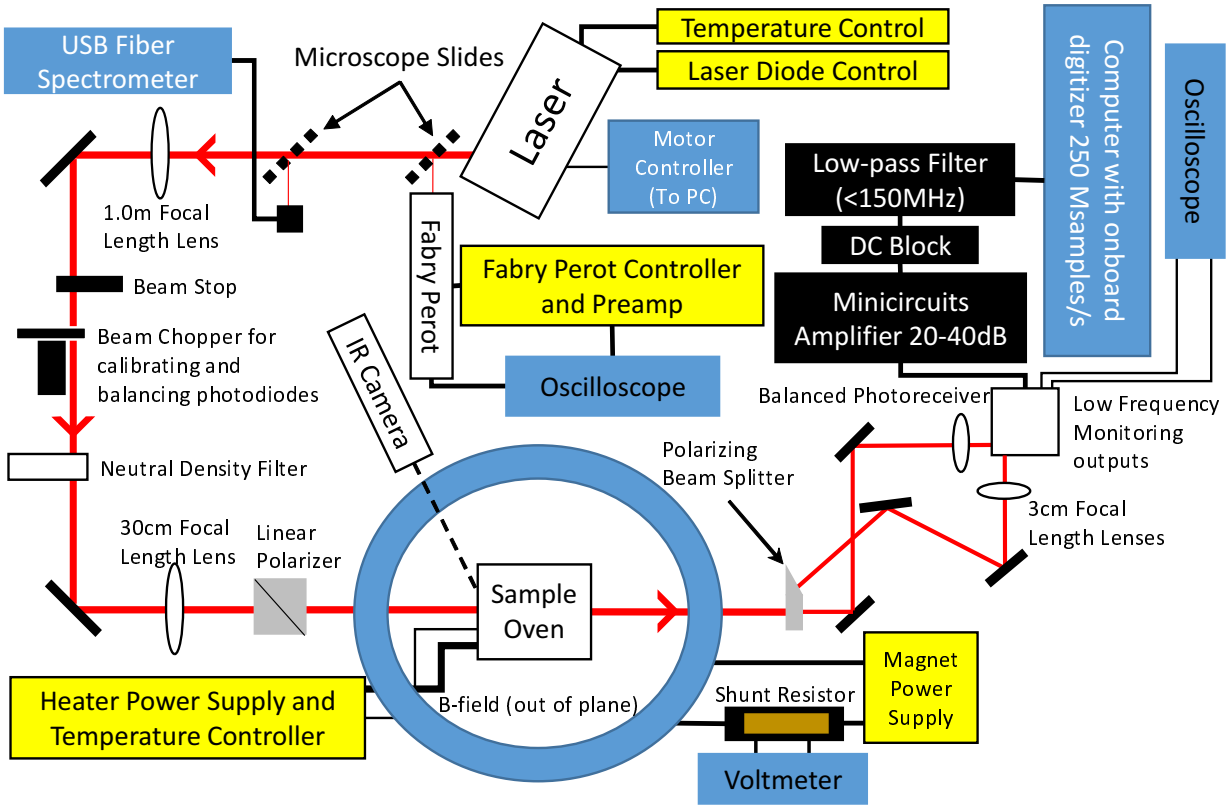

Figure 1: Schematic of spin noise apparatus. Microscope slides are used as cheap beam samplers. A glass cell containing Rb vapor is located inside of the sample oven. Data are collected and analyzed in LabView.

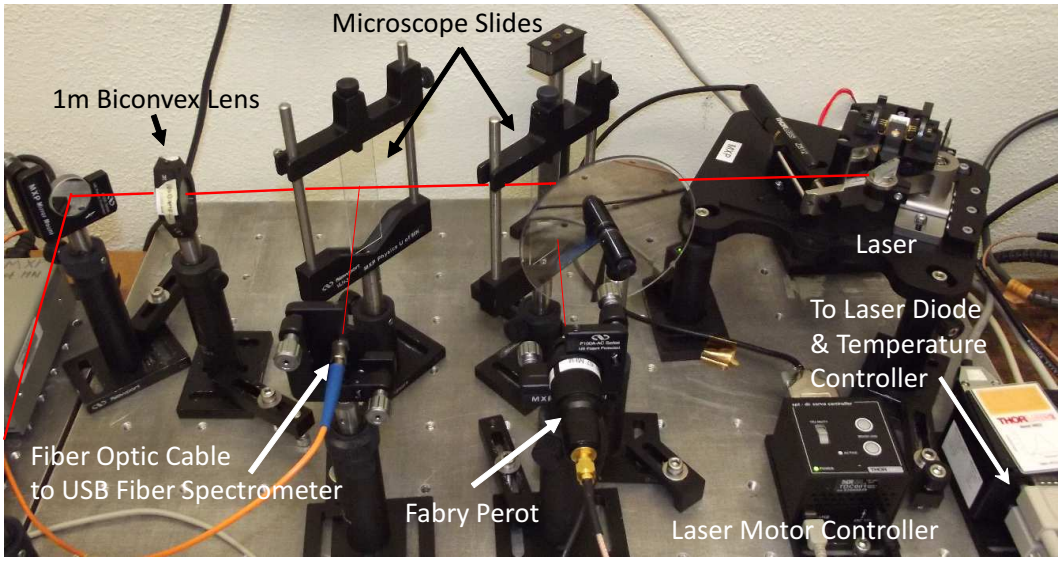

Figure 2: Laser and first leg of the laser's path. The laser motor, which is controlled by software, is used to adjust the wavelength. The fiber goes to a USB spectrometer, which is used for coarse tuning. The Fabry-Perot etalon is used for fine tuning (below 100 GHz) and monitoring laser stability.

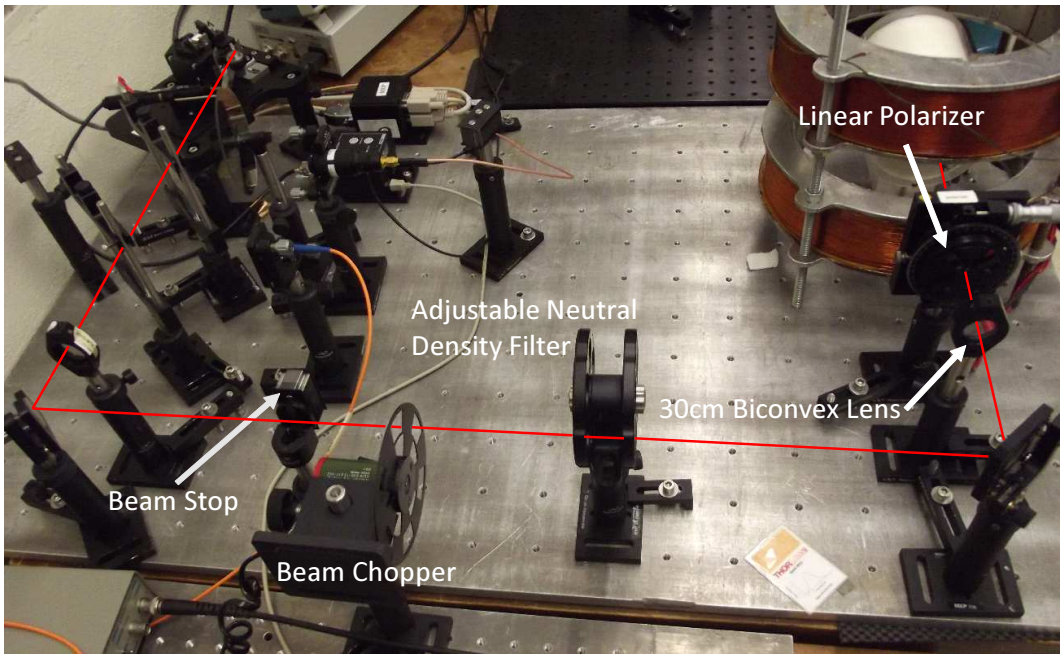

Figure 3: The second leg of the laser path. The beam stop is used when a noise spectrum without laser light incident on the photodiode (i.e. a dark power spectrum) is needed. The chopper is only used when aligning the polarization bridge and zeroing the balanced receiver. An adjustable neutral density filter is used to control the incident power. In this case, a calcite polarizer is used to create linear polarized light. An ordinary dichroic polarizer will work as well.

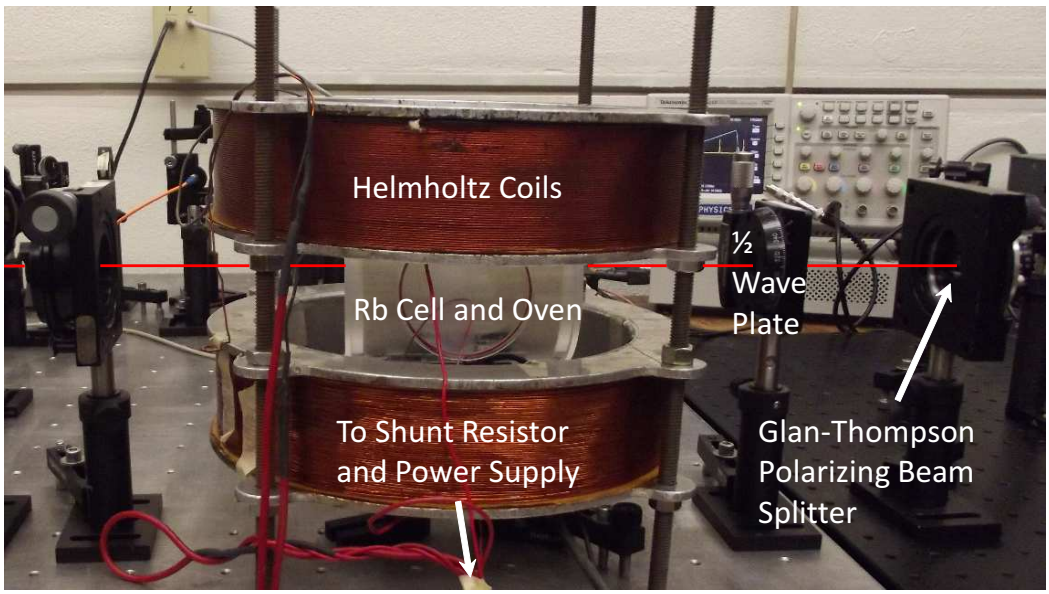

Figure 4: The third leg of the laser beam. The beam passes through the Rb vapor with an applied magnetic field. The 1/2 wave plate is optional. It can be adjusted instead of the linear polarizer to rotate the plane of polarization and balance the photodiode bridge without any loss of incident power. Finally the laser light reaches the polarizing beam splitter.

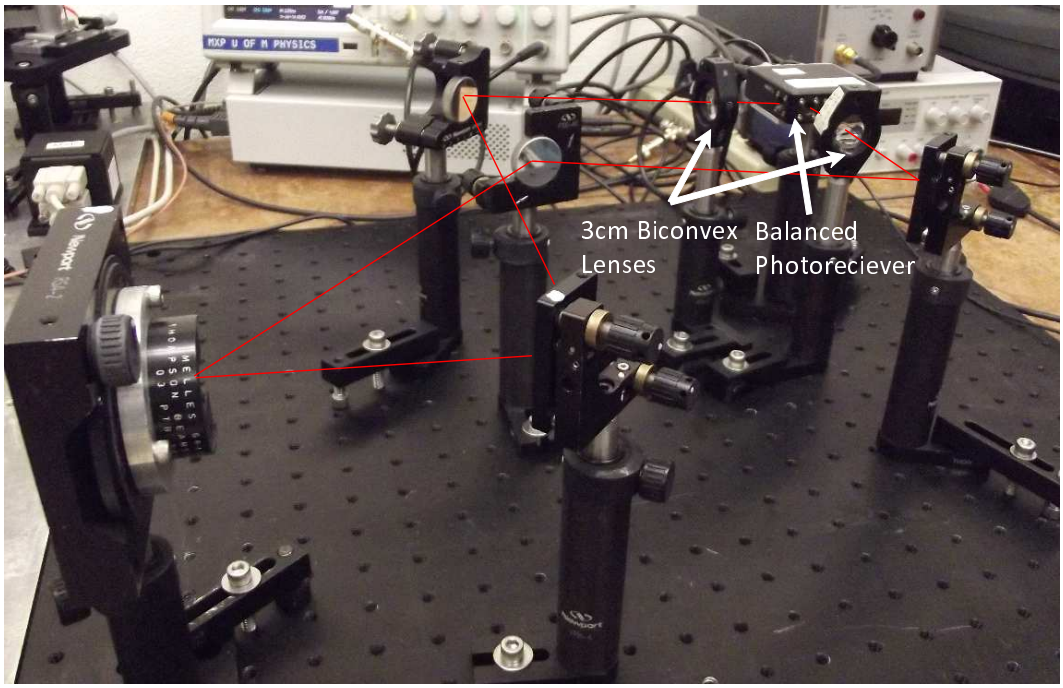

Figure 5: Final leg of the laser path. Here the vertically and horizontally polarized light is incident on the balanced photoreceiver. The two lenses before the receiver focus the beams to spots smaller than the active area of the photodiodes.

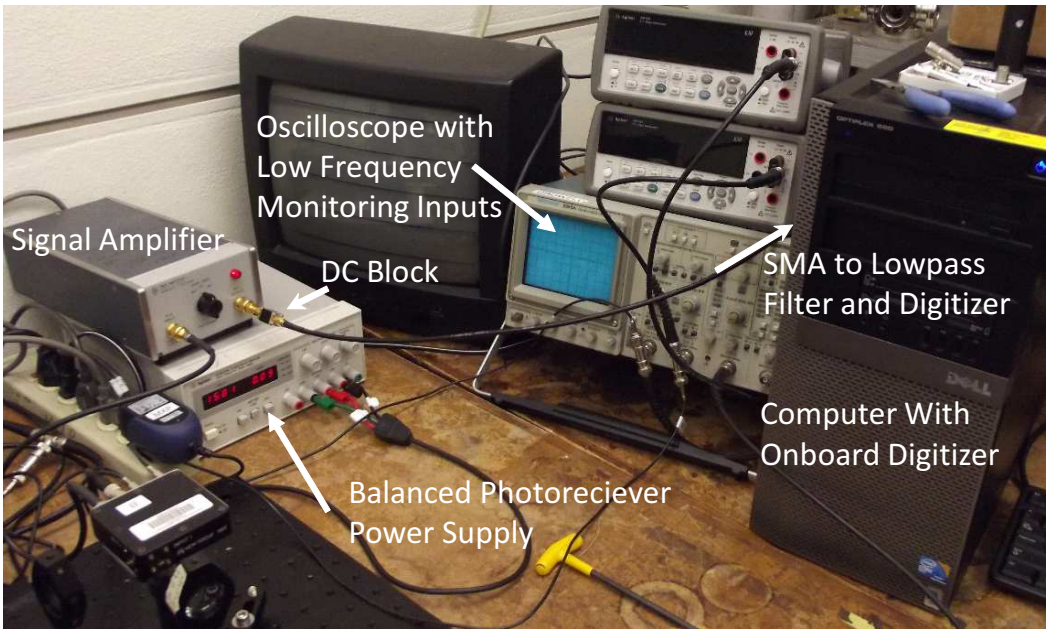

Figure 6: After the voltage signal from the difference channel leaves the balanced receiver, it is amplified and filtered before reaching the digitizer. Not shown is the low pass filter connected to the input of the digitizer to roll off high-frequency components that are otherwise aliased into the frequency range of the measurement. Depending on your digitizer, this feature may be available in software. Also pictured here are the oscilloscope and voltmeters used to monitor the two low-frequency channels of the balanced receiver.

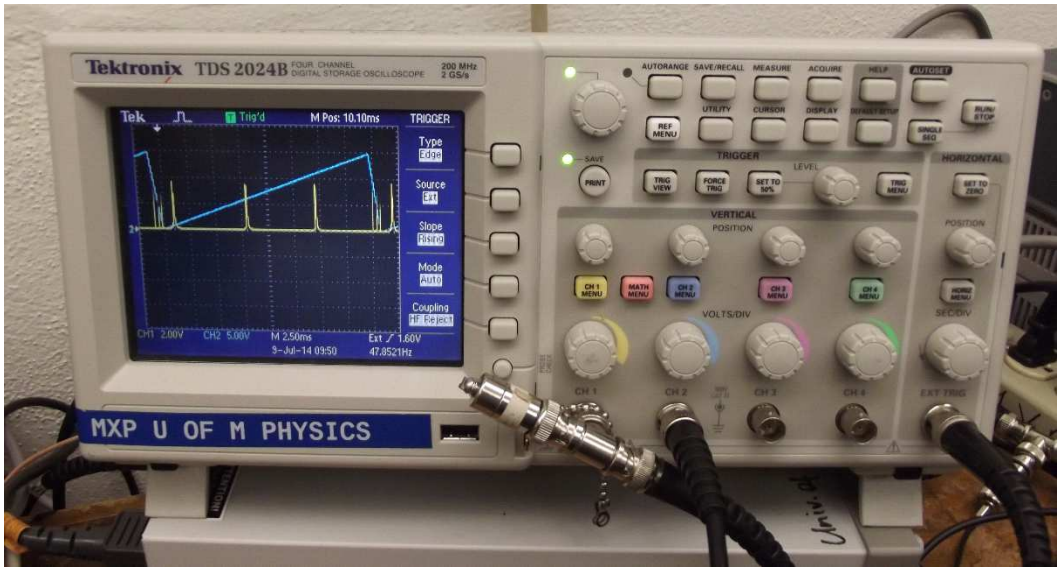

Figure 7: Typical output from the Fabry Perot spectrometer. The periodic sharp peaks with little drift indicate single mode operation of laser.

Equipment List

Optional: Ocean Optics Red Tide USB 650 Laser Spectrometer and Software
Optional: Stanford Research Model SR 540 Beam Chopper and Controller
Thor Labs TLK-L780M Free-Space Laser Kit
Thor Labs LDC 500 Laser Diode Controller
Thor Labs TEC 2000 Temperature Controller
Laser Power Meter
Dichroic Polarizer *OR* optionally Calcite Polarizer
Optional: 1/2 Wave Plate
Thor Labs SA210-5B Scanning Fabry-Perot Interferometer 535-820nm
Thor Labs SA 201 Spectrum Analyzer Controller
New Focus 1607 Balanced Photoreciever 320-1000nm, 650 MHz Bandwidth
Power Supply for Balanced Photoreciever
Assorted Mirrors and Bifocal lenses
Adjustable Neutral Density Filter
Microscope Slides and Mounts
Helmholtz Coils
Kepco DC Power Supply 0-100V 0-1A (for Helmholtz coils)
K and Rb vapor cells are available from Precision Glassblowing: http://www.precisionglassblowing.com/
Rb Cell and Oven are also available as part of the TeachSpin Optical Pumping Apparatus
1-2 Voltmeters
1-2 Oscilloscopes
100 mΩ Shunt resistor
HP 461A Amplifier with Adjustable Gain 20,40dB *OR* 1-2 Minicircuits ZFL-1000LN 1000 MHz 20dB Gain Amplifier
Picosecond Pulse Labs 5500A DC Block (can be replaced with any in-line blocking capacitor)
Assorted Minicircuits BLP-XXX BNC Low Pass Filters
SMA Cables
BNC Cables
Optional: Video Camera and Monitor to use as infrared viewer
Computer with LabView
NI PCI-5114 250 MSamples/s, 8-Bit Digitizer
Aluminum optical breadboard

Lab Manual: Spin Noise Spectroscopy in Rb

Introduction

The classic atomic spectroscopy experiment is perturbative. Atomic transitions are identified through absorption or emission of light, either of which requires a departure of the system from equilibrium. Optical pumping of alkali atoms, which is one of the most dramatic demonstrations of high-resolution spectroscopy in an undergraduate laboratory, goes a step further, in that the optical pumping process leads to a significant redistribution in the ground-state populations of an alkali atom, such as Rb. This experiment introduces a subtle but powerful concept: noise spectroscopy. Instead of measuring the response of a system to an external perturbation, we "listen" to fluctuations of the system in thermal equilibrium. The concept is illustrated using the hyperfine-split $^2S_{1/2}$ ground state of Rb or K.

At a global level, the experiment is very simple. A bath of spins has an average magnetization of zero. A small magnetic field is applied. Any fluctuation of the spin precesses around this magnetic field with a characteristic Larmor frequency, Ω_L. For the range of magnetic fields of interest in this experiment, the Larmor frequencies fall between 1 and 125 MHz. A key fact is that if a beam of polarized light is passed through the ensemble and tuned near an optical transition that depends on spin, the Faraday rotation of the optical polarization vector will be modulated by the spin fluctuations [1]. In a finite magnetic field, the modulation occurs at the Larmor frequency. By reading out the polarization signal in the time domain and then taking a Fourier power spectrum (FPS), the spin noise will appear as a peak in the spectrum at Ω_L. If there are multiple transitions with different Larmor frequencies, the FPS of the noise signal can be used to measure the spectrum.

This lab can be used to teach any number of concepts, and the instructor will want to select exactly which of these to emphasize. The roots of the experiment lie in the fluctuation-dissipation theorem [2]. The intent is to illustrate only that an ensemble of atoms with an average magnetization of zero has a magnetic moment that is constantly fluctuating about zero, and the characteristic size of the fluctuating moment scales as $\sqrt{N}$, where N is the number of spins in the ensemble. No advanced mathematics is required to understand this point, and a more rigorous treatment of the fluctuation-dissipation theorem is not necessary.

The second important point is the demonstration of a non-perturbative probe, which in this experiment will be off-resonant Faraday rotation. We assume that the student is familiar with conventional absorption and emission spectroscopy. It is much less obvious how to probe a system without absorption or emission. The tool of choice is Faraday rotation, which has the benefit of being sensitive to spin and of being measurable at significant detuning from resonance.

The third point which can be emphasized is the conversion from time-domain to frequency-domain data. This allows for discussion of the sampling theorem, and the need for an efficient calculation of the FPS. The student will learn that noise spectroscopy requires the accumulation of large amounts of data, and one must calculate the Fourier transform and average power spectrum at a rate which matches the rate of data acquisition. The level of

challenge can be made commensurate with the experimental goals. For example, measuring Larmor frequencies of a few MHz can be executed with a generic data acquisition card and Labview programming. At several hundred MHz, the challenge is significantly increased.

Finally, there is the spectroscopy. It is rather remarkable that the Fourier power spectrum of a spin noise signal can provide a complete spectrum of the hyperfine transitions in the ground state of the alkalis. Understanding this spectrum requires a full development of the Breit-Rabi formalism. Because this is covered extensively in the background literature for experiments such as optical pumping [3], this manual will not address the atomic physics of the alkalis in detail. Essentially, we will assume the validity of the Breit-Rabi formula.

Theory

As noted above, the main point of this experiment is to obtain spectroscopic information from fluctuations of an ensemble of alkali atoms in thermal equilibrium. In this case, the fluctuating quantity of interest is the total spin of the ensemble. At the magnetic fields used in this experiment, the average spin of a gas of alkali atoms is zero. In practice, any particular measurement of a single component of the average spin of the ensemble will return a value of order $\sqrt{N}\hbar/2$, where N is the total number of atoms. At the cell temperatures, beam diameters, and cell length that we use in this experiment, we sample approximately 10^9 atoms. In a small magnetic field, the fluctuation-dissipation theorem requires that the spectrum of fluctuations is proportional to the magnetic susceptibility spectrum, [2] which is what one would measure as an absorption spectrum in a standard spin resonance experiment.

In practice, obtaining a true susceptibility spectrum is not easy. In any resonance experiment, it is extremely difficult to avoid saturating the spin system, and optical techniques (e.g. optical pumping or absorption) typically require a perturbation in the occupancy of the various atomic states. In principle, these problems are avoided in a noise spectroscopy experiment *provided* that whatever is being used to probe the system couples only weakly to it. This is accomplished by exploiting the fact that a magnetically active optical transition will, in the presence of spin-orbit coupling, couple to the polarization of light [1]. For example, each of the optically active $\Delta m_f = \pm 1$ transitions between the $^2S_{1/2}$ and $^2P_{1/2}$ or $^2P_{3/2}$ states of the alkalis yields an absorption peak that is actually a superposition of absorption peaks for left and right circularly polarized light. As the wavelength of light is tuned through the absorption maximum, the real part of the index of refraction n passes through zero, with extrema occurring on either side of the absorption maximum. This dispersive response (see Fig. 8) decays very slowly with respect to frequency. As a function of detuning $\Delta = \Omega - \Omega_0$, where Ω_0 is the frequency of the absorption peak, n varies as $1/\Delta$. In contrast, the optical absorption $\alpha \sim 1/\Delta^2$. Because the index of refraction decays more slowly with detuning than the absorption, one can measure the dispersion in the optical response in a region where the absorption is small. It can be shown that the difference in the indices of refraction of right and left circularly polarized light is proportional to the rotation of the plane of polarization of linearly polarized light: *i.e.,* the Faraday rotation Θ_F.[4]

We will therefore measure the Faraday rotation at a frequency "sufficiently far away" from

the peak optical absorption frequency. In practice the detuning will be from 10 - 100 GHz. Keep in mind that the actual optical absorption peak (and even the laser line) is much broader than any of the spectral features we are trying to resolve. The spectral information in this experiment comes from fluctuations in the Faraday rotation (in the MHz range) measured at a fixed optical wavelength. In practice, frequency resolution of a few kHz is possible at moderate levels of detuning.

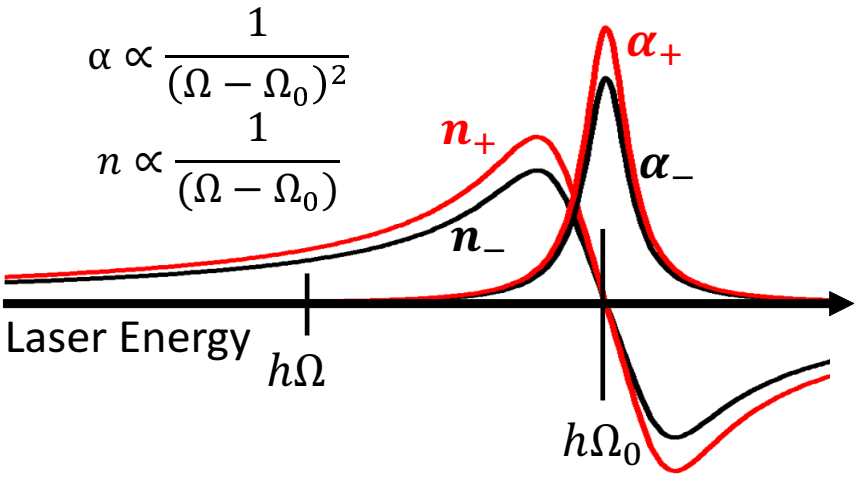

Figure 8: The relationship between absorption (α) and dispersion (n) with respect to frequency. The $\pm$ refers to the spin up and spin down states. Ω_0 is the frequency of the absorption peak, and Ω is the probe laser frequency.

The atomic physics of this experiment is essentially identical to that required to understand the standard optical pumping experiment carried out routinely in undergraduate laboratories. In a small applied field B, the spin noise will have peaks at frequencies Ω_L corresponding to the weak-field Zeeman splitting:

$$h\Omega_L = g_F \mu_B B, \tag{1}$$

where g_F is the Landé g-factor for the states with total angular quantum number F, and μ_B is the Bohr magneton. In our case, we are considering only the ground state of an akali atom with $S = 1/2$, $L = 0$, $J = L + S = 1/2$. The reader should consult a standard reference [3] for a treatment of the atomic physics of the alkalis. For ^{85}Rb, $I = 5/2$, and the possible values of the total angular momentum $F = |I \pm J|$ are 2 and 3. For ^{87}Rb, $I = 3/2$, and the possible values for F are 1 and 2. The respective g-factors are $g_F = 1/3$ for ^{85}Rb and $g_F = 1/2$ for ^{87}Rb. For natural Rb, there will be two low-field peaks. The ^{85}Rb peak originates from 12 degenerate levels with 10 allowed $\Delta m_F = \pm 1$ transitions, while the ^{87}Rb peak originates from 8 degenerate levels with 6 allowed transitions.

As the field increases, the degenerate levels split due to the hyperfine interaction. For the $J = 1/2$ ground state, the energies of all levels are given by the Breit-Rabi formula:

$$E_{F,m_F} = \frac{-\Delta_{hf}}{2(2I+1)} + g_I \mu_B B m_F \pm \frac{\Delta_{hf}}{2}\sqrt{1 + \frac{4m_F}{2I+1}x + x^2}, \tag{2}$$

where

$$x = \frac{(g_J - g_I)\mu_B B}{\Delta_{hf}},$$

Δ_{hf} is the hyperfine splitting between the two F states at zero field, m_F is the magnetic quantum number, g_I is the nuclear g-factor, g_J is the electron g-factor, and the positive and negative sign are used in the upper ($F = I + 1/2$) and lower ($F = I - 1/2$) manifolds respectively. With increasing field, the quadratic Zeeman effect due to the last term in Eq. 2 breaks the degeneracies and all distinct transitions allowed by the $\Delta m_F = \pm 1$ selection rule within each manifold (i.e. $\Delta F = 0$) can be resolved (see Fig. 9). At higher frequencies, the $\Delta F = \pm 1$ transitions between the two manifolds can also be observed. This is not practical (with our apparatus) for Rb, where the hyperfine splittings are 3.0 and 6.8 GHz for the two isotopes. With a 2 GHz digitizer, we have been able to observe the $\Delta F = 1$ transitions in ^{39}K and ^{41}K, for which Δ_{hf} is less than 500 MHz in both cases.

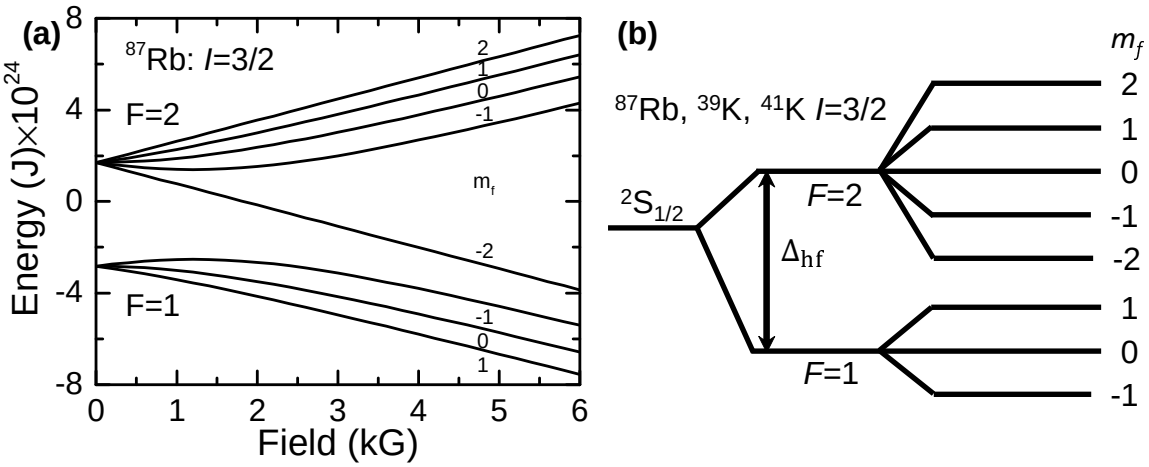

Figure 9: (a) Plot of Zeeman energies for $I = 3/2$ atoms. Spin noise peaks occur at frequencies equivalent to the energy between transitions allowed by the optical selection rules. (b) Schematic of the energy levels for $I = 3/2$ isotopes ($F = I \pm 1/2$).

Equipment and Experimental Setup

The basic experiment follows closely the one described in Ref. [5]. An extremely low-frequency version and rather limited version of the experiment is described in Ref. [6]. Figs. 1 & 10 show the schematic of the experimental set up. Laser light is provided by a tunable, open cavity laser (Thor Labs Model TLK-L780M Free-Space Laser Kit). The laser is detuned by ∼30 GHz from a particular optical transition in Rb (for example the D2 transition which is ∼780nm) to minimize absorption and still allow for a measurable Faraday rotation. The light is linearly polarized. The laser light is sent through a Rb vapor cell, which is operated at a temperature of 100-200 degrees Celsius. The temperature is used to control the density of atoms in the vapor, which depends exponentially on the cell temperature. A buffer gas of Ne or N_2 at a pressure of 50 Torr is essential to enhance the

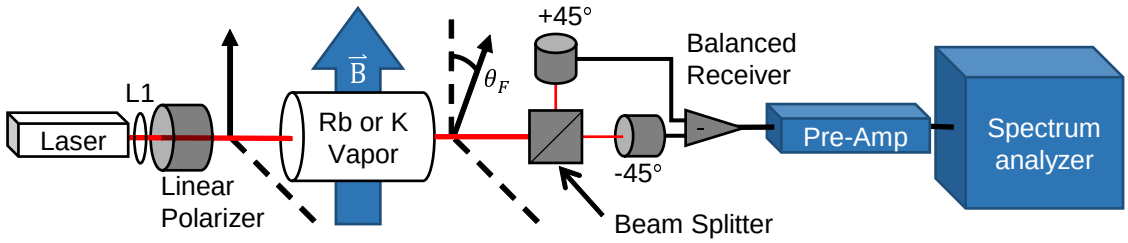

Figure 10: Simplified experimental schematic. An external cavity, adjustable wavelength laser is used for the source. L1 is a long focal length lens used to focus the light into the cavity. The Rb vapor is contained in a glass cell heated to 100°C. The applied field is produced by Helmholtz coils. The output of the balanced receiver is the difference in intensity of the individual photodiodes and is proportional to the Faraday rotation. The signal is digitized and analyzed in real time using FFT provided by LabView.

collision rate and increase the time over which a spin fluctuation interacts with the light beam. In the absence of a buffer gas, the magnetic transitions would be broad and unobservable. All of the required features of the vapor cell, including the buffer gas, are provided as part of the TeachSpin optical pumping apparatus. The 100°C temperature achievable with the TeachSpin oven is sufficient for experiments on Rb. We built our own oven for the experiments on K, where higher temperatures (up to 200°C) are required. Precision Glass Blowing (http://www.precisionglassblowing.com/) can provide standard alkali vapor cells with a buffer gas pressure that you specify.

There is only one other optical component required on the incoming light path: the focusing lens L1, which is required to achieve beam diameters less than 0.5 mm passing through the cell. The key point is that the Faraday rotation signal will scale with the fluctuating magnetization, which is proportional to the square root of the number of spins in the volume traversed by the laser beam divided by the sample volume [5]. This ratio is proportional to $1/\sqrt{A}$, where A is the cross-sectional area of the laser beam. In other words, the Faraday noise signal increases as the beam area decreases. The noise *power* will decrease as $1/A$.

A transverse field of less than 100 Gauss (0.01 Tesla) is supplied by Helmholtz coils. Note that this experiment probes fluctuations of the magnetization and is sensitive to the spin oriented along the optical axis. The geometry is different from an ordinary Faraday rotation experiment, in which there is a static magnetization parallel to the optical axis.

Stability and homogeneity of the magnetic field are particularly important. The required resolution is of the order of a few kHZ at 20 MHz, and so the magnetic field must be stable and homogeneous to better than 1 part in 1000. The Helmholtz coils provide the required homogeneity, although care must be taken to make sure all components (including the optical breadboard) are non-magnetic. Many power supplies will oscillate with large inductive loads, and it is wise to monitor the ac voltage across the Helmholtz coils. A capacitor can be placed in parallel to reduce ripple to an acceptable level. If one wishes to probe higher fields, drift will become important, particularly when the data collection times are long. In that case, a current-regulated power supply is essential.

After passing through the Rb vapor cell, the laser beam is incident on a polarizing beam splitter which splits the linearly polarized light into vertically and horizontally polarized components. The two separate beams are incident on a balanced photoreceiver. The photoreceiver takes the difference in the two photodiode currents, amplifies it, and converts it into a voltage. The voltage is directly proportional to the Faraday rotation angle. Most commercial digitizers have ranges that can be set on the order of tens of millivolts. The signal from the balanced photoreceiver is on the order of hundreds of nanovolts and therefore must be amplified. Two models that we found worked well are the HP 461A Amplifier (no longer in production) and the Minicircuits ZFL-1000LN Amplifier. For the balanced photoreceiver used (NewFocus Model 1607) we needed 20dB of gain with input powers of order 1 mW. A dc blocking capacitor may be required to protect the front end of the digitizer. The signal is then sent to LabView to calculate the FPS (Power Spectrum in LabView) and average the spectra over time. A large number (roughly 100,000 averages) of averaging cycles are necessary to achieve reasonable signal to noise. For this reason care should be taken with the LabView programming to create as efficient an averaging protocol as possible.

LabView Programming Notes

There are a few things to note before considering the noise spectrum in detail. In principle, the digitizer card "records" fluctuations of the polarization in the time domain, and we simply take the FPS in order to determine the spectrum. In practice, one has control over many parameters that influence the success of the experiment. Note that high amplitude precision is not required. An 8-bit digitizer is sufficient. The gain of the input channel should be set to maximize the dynamic range used by the digitizer. The sampling rate should be set at twice the maximum frequency you need to measure (Nyquist theorem). The length of time required to collect each sample record will be set by the frequency resolution required. For the data shown here, records of 8,192-16,384 bytes are sufficient. Finally, observing the noise spectrum requires many measurements. At sampling rates of 50 MHz, it is not uncommon to average spectra over 10 minutes of laboratory time. A large number (roughly 100,000 averages in the frequency domain) of spectra are necessary to achieve reasonable signal to noise.

The basic LabView code for obtaining data, applying the FPS, and averaging the result is shown in Fig. 11. Data are acquired, a Fourier transform is applied, and the result is added to the previous spectrum. This is repeated a set number of times and the resulting array is returned. Depending on the digitizer and processing speed of the computer, this basic program may meet the needs of the experiment.

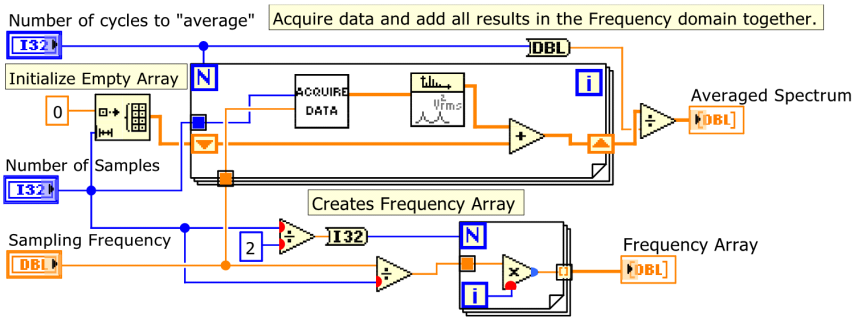

Figure 11: Basic LabView programming diagram.

This basic program may not function fast enough to acquire the necessary number of averages. If that is the case there are two possible problems: the digitizer takes too long to process data and move it to the computer, or the computer takes too long to process incoming data. Both cause a slowdown in the throughput or duty cycle. The duty cycle is defined as the actual live time during which data is acquired (based on the number of samples and sampling rate) divided by the actual time of data acquisition and analysis. Provided in Fig. 12 is our calculated duty cycle for different sampling rates. Your setup may provide numbers exceeding these. They are provided as an example of reasonable program efficiency.

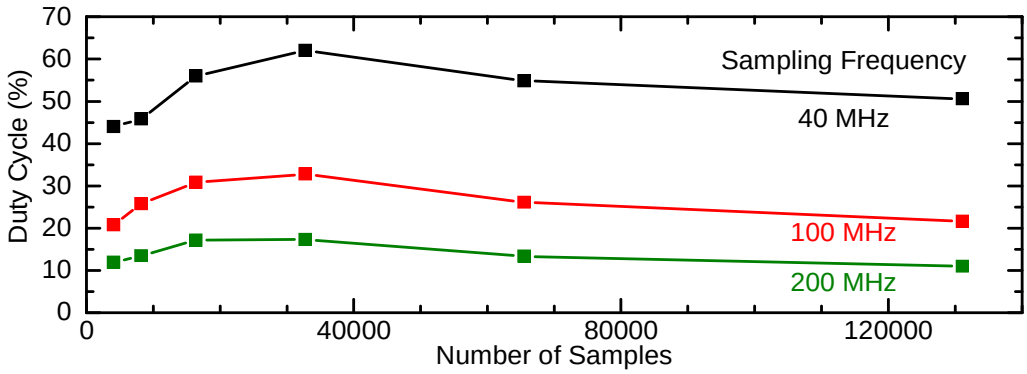

Figure 12: Duty cycle of our set-up achieved for different number of samples and sampling frequencies. All values were found from doing 20,000 averages.

An alternative more efficient programming scheme is outlined in Fig. 13. This diagram demonstrates two techniques to increase efficiency. First it has separated the data acquisition loop and the data analysis loop. LabView has the ability to process events in parallel (assuming the computer you are using has multiple cores). This is done by simply creating two separate loops. The second technique employs the Queue architecture. A queue is created with a set number of empty arrays. Elements are *Enqueued* adding them to the next available spot in the array. The two data analysis loops then *Dequeue* elements for the application of the FPS. The VI schematic pictured in Fig. 13 is optimized for a computer that could not keep up with the data acquisition. For this reason there is also a case structure that checks the number of elements in the queue. If that number exceeds 1,498, it ceases data

acquisition (thus freeing up processing power) until the number in the queue is under 200. This was determined to be a reasonably efficient method for the particular data acquisition card and computer used. It should be emphasized, however, that the advanced techniques discussed in this paragraph are likely not necessary for measurements below 40 MHz.

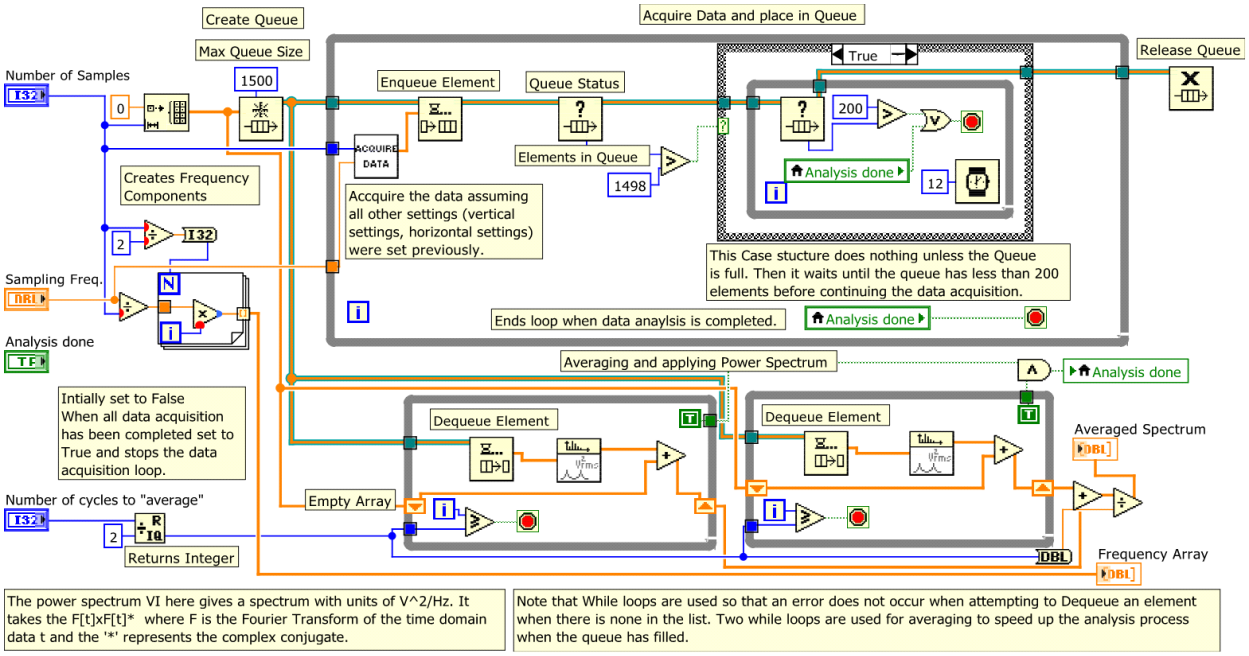

Figure 13: A more advanced method for acquiring and analyzing data.

Laser Alignment and Tuning

There are a few basic requirements of the laser used for this spin noise experiment. The laser must be able to reach a wavelength of 794nm or 780nm (D1 and D2 optical transitions in Rb respectively). The linewidth and absolute stability are not critical (a few MHz will do), but the laser should operate on a single mode. The wavelength can be checked on a coarse scale using a USB-based fiber spectrometer. The laser must be able to tune smoothly through the atomic transition with minimal mode hopping. A scanning Fabry-Perot etalon can be used to determine the stability of the laser. Narrow, well defined peaks at constant intervals (one per free spectral range of the Fabry-Perot etalon) should be seen with little drift if the laser is operating correctly (see Fig. 7).

Rb Cell, Sample Oven and Magnet Calibration

The buffered Rb cell and oven can be borrowed from the TeachSpin optical pumping apparatus. The cell should be heated to approximately 100 °C. A crude homemade oven can also be fashioned. The only significant detail is to limit radiative cooling through the ends of the cell, which will cause Rb to plate out on the end windows. If this occurs, a heat gun can be used to remove the condensed metal. Some parts of the cell may become permanently

discolored. This is the motivation for two mirrors being placed between the oven and laser. Using these two mirrors, the beam can be "walked" across the cell without repositioning of the laser.

Calibration of the magnet is accomplished using a shunt resistor in series with the magnet power supply. Once the current is known, two options exist for determining the magnetic field (unless you really trust the geometry of your Helmholtz coils). First, a Gauss meter can be positioned at the location of the cell and field readings with respect to current can be made. This method's accuracy depends on the precision of the Gauss meter. An alternative method is to take noise spectrum measurements with only a small current applied to the magnet. It should be in the regime where only single noise peaks are visible. Using Eq. 1, the applied current, the known g-factors, and noise peak locations, a relationship between applied field and current can be made. With the low field calibration and the linear relationship between applied current and the resulting field, extrapolation to higher fields can be made. As noted above, magnetic material can both limit the homogeneity of the field and impact the calibration.

Beam Size, Alignment and Balancing of the Balanced Receiver

As mentioned previously a small beam diameter is imperative in order to obtain a good signal to noise ratio. This task can be accomplished with one or two long focal length (1 meter) lenses placed before the cell. The reason for the long focal length is to ensure the beam diameter is constant inside the cell.

After the linearly polarized light has passed through the Rb cell and polarizing beam splitter, the light is incident on the balanced photoreceiver. The primary output of the balanced photoreceiver is a high frequency (650 MHz bandwidth) difference channel. The voltage at this output is proportional to the difference of the photocurrents from each diode. Low frequency outputs are also available to monitor the photocurrent in each photodiode as well as the difference of the two photocurrents. Shot-noise limited performance is essential in order to see spin noise. Therefore, you will likely be using a laser power (on the order of 1 mW) that is near the saturation threshold of the receiver. A neutral density filter can be positioned before the linear polarizer to reduce the laser power without needing to make laser adjustments.

A key component of the experiment is the extraordinary common mode rejection and sensitivity to small polarization rotations provided by the balanced receiver. The vertically and horizontally polarized beams exiting the polarizing beam splitter are focused (using a short 3-9cm focal length lens) to spots smaller than the active area of the photodiodes. To test for proper focus, it should be possible to make slight adjustments to the position of the last mirror without significant changes in the low-frequency monitor output. A sharp drop-off should occur as the focused laser leaves the diode. Using an optical chopper allows for the monitor outputs to be viewed as square waves on an oscilloscope. After the voltage from each diode has been maximized (through mirror and lens adjustments), balancing of the photoreceiver can occur. This task can be completed by adjusting the orientation of the

linear polarizer. If a half-wave plate is available, it can be used instead. If properly balanced, the output of the low frequency difference channel should fluctuate about zero volts. This final calibration step should be repeated every few runs to ensure the best signal to noise possible.

Finding Detuning from Optical Resonance

Because of the buffer gas in the cell, the D1 and D2 transitions are each broadened into lines that are several GHz wide. Each transition has a characteristic absorption maximum. Two methods can be employed to find the optical resonance. In the first an infrared camera is aimed at the cell while sweeping the laser frequency. The cell will glow when optical resonance occurs. The second more precise method is to sweep laser frequency while monitoring one of the low frequency outputs of either photodiode. On resonance, there will be a dip in the photodiode voltage. At higher cell temperatures (e.g., 100 ° C), the absorption can be nearly complete. Once the absorption peak is found, the laser can be detuned to a point at which twenty to zero percent of the light is absorbed. This should be somewhere around 30-60 GHz from the center of the absorption line. If mode hopping occurs one may try the opposite side of the absorption center.

Data Taking Procedure

The first test to perform before taking data is to take a power spectrum with and without laser light incident on the photodiodes. If everything is working properly the difference between these two spectra, which is the shot noise power, should scale linearly with laser power. A typical case is shown in Fig. 14. The shot noise must be easily resolvable in order to observe spin noise. At a laser power of 1 mW, the shot noise should be clearly visible after averaging 5,000 spectra.

Due to the non-constant gain of the amplifiers and photodiodes there will be a frequency-dependent background. For this reason, the raw shot-noise power spectrum is not actually white (flat) in character. We found that the most practical way to remove the dark and shot noise backgrounds is to take the difference of spectra with and without magnetic field. The two cases can be subtracted and an almost completely flat noise spectrum will be obtained except for the spin-dependent noise peaks of interest (see Fig. 14).

There are two regimes in which it is easy to interpret the noise spectra. At low fields (less than 10 Gauss), only a single noise peak is visible for each isotope of Rb. At high fields, the nuclear Zeeman and quadratic Zeeman effects allow all $\Delta m = 1$ peaks to be resolved. The intermediate regime is more difficult to analyze because the peaks are too close together.

The parameters to use for the digitizer vary depending on the field regime, which determines the frequency, and the desired precision. For low field measurements a sampling rate of 20 MHz with 16,384 samples is more than sufficient. Decreasing the number of samples will decrease the time of acquisition but decrease the frequency resolution. At higher fields,

a sampling rate of 200 MHz with 65,536 samples was used. Note that the Fast Fourier Transform requires the number of samples always be a power of two. For the data shown below, 100,000-300,000 averages were completed, with a single run taking around 8 minutes.

Data Analysis

After the subtraction of the noise spectra with and without magnetic field, the spin noise spectrum is obtained (black data set in Fig. 14). A non-linear least squares fit can be made to determine the location, width, and amplitudes of the peaks. Data analysis software such as Origin can be used to make this process quite efficient. From this information, plots of peak frequencies as a function of magnetic field can be made. These are shown in Fig. 15 (b) & (d), in which the solid lines are the expected frequencies based on the Breit-Rabi formula. Alternatively, the data can be fit with the Breit-Rabi formula using the hyperfine splitting as a fitting parameter, and the values of the hyperfine splitting shown in Table 1 can be determined.

As mentioned previously, the spin noise amplitude scales as the $\sqrt{N}$, where N is the number of atoms, and so the integrated spin noise power should scale with N. This provides a simple means of determining the isotopic abundance ratio for the Rb cell. The area under the low-field noise peak is determined for each isotope by integrating the FPS. The ratio of the areas under the peaks for each isotope is the ratio of the concentrations. This procedure works best at low field where there are only single peaks for each isotope.

This manual outlines some of the basic spectroscopic parameters that can be determined from spin noise spectroscopy in Rb vapor. The dependence of the noise power on temperature (density), beam detuning, and beam area can also be made as outlined in Ref. [5]. With slightly more bandwidth (1 GHz), and a higher temperature oven (up to 200 °C) measurements on ^{39}K or ^{41}K are also possible. Because the hyperfine splittings in these isotopes are much smaller, the $\Delta F = 1$ transitions can be observed directly,[5, 7] with a resolution limited only by sampling considerations (see data in Table 1). Finally, it is possible for very advanced students to compare the relative magnitudes of the spin noise peaks for different transitions with the predictions of quantum mechanics.[7]

Sample Data

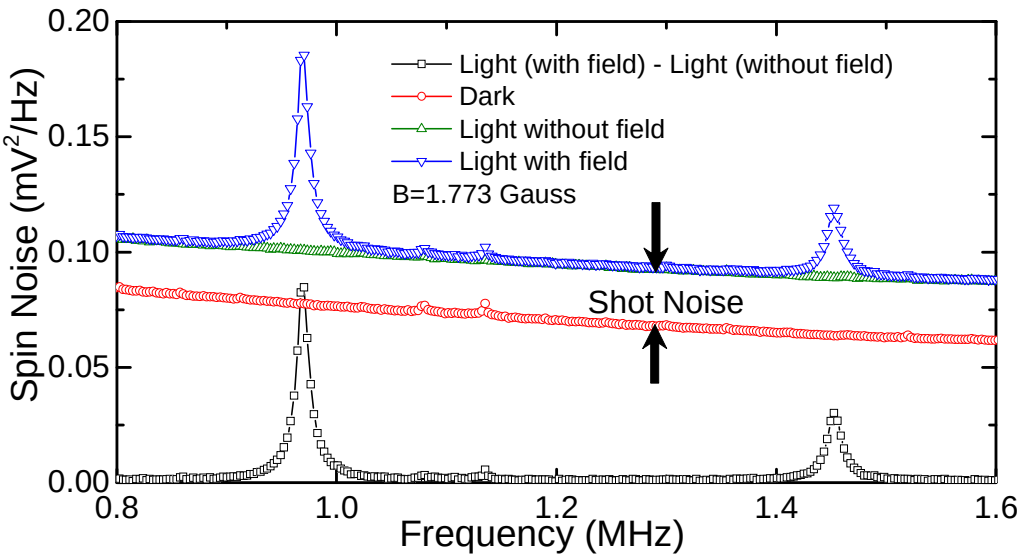

Figure 14: The low field Rb spin noise peaks. The difference between the red and green curves is the shot noise background. The subtraction of the "Light without field" curve from the "Light with field" curve was used for data analysis. Data taken at 30 GHz laser detuning (10% laser absorption), 1.0 mW beam power, 373 K, 10 MHz sampling frequency, 4,096 samples, and 300,000 averages (a single spectrum took about 3 minutes). Note that the spin noise signal displayed here has not been corrected for the frequency dependent gain of the amplifiers.

Δ_{hf} - Zeeman	^{85}Rb [8]	^{87}Rb [9]	^{39}K [8]	^{41}K [8]
Expected	3.0357 GHz	6.834 GHz	461.71972 MHz	254.01387 MHz
Measured	3.00 ± 0.01 GHz	6.8 ± 0.1 GHz	468 ± 6 MHz	256 ± 4 MHz
Δ_{hf} -Hyperfine	^{87}Rb	^{85}Rb	^{39}K	^{41}K
Expected	-	-	461.71972 MHz	254.01387 MHz
Measured	-	-	461.720 ± 0.005 MHz	254.030 ± 0.002 MHz
Nuclear g-factor	^{85}Rb [8]	^{87}Rb [8]	Abundance Ratio	^{85}Rb/^{87}Rb [10]
Expected	2.9364×10^{-4}	9.9514×10^{-4}	Expected	1.610
Measured	$(2.80 \pm 0.01)10^{-4}$	$(9.970 \pm 0.005)10^{-4}$	Measured	1.62 ± 0.01

Table 1: Results are included here to give an idea of the accuracy and precision to which parameter values can be determined. "Zeeman" refers to fitting done to the low field Zeeman noise peaks ($\Delta F = 0$ transitions) and "Hyperfine" refers to hyperfine splitting extracted directly from the frequencies of the $\Delta F = 1$ transitions. Note that for Rb the hyperfine spin noise peaks were outside the frequency range of our digitizers. All uncertainties are standard errors. Expected values come from the reference next to the given isotope. Ref. [11] Also provides a good reference for Rb data and basic optical transition theory. All other physical constants used are from Ref. [12].

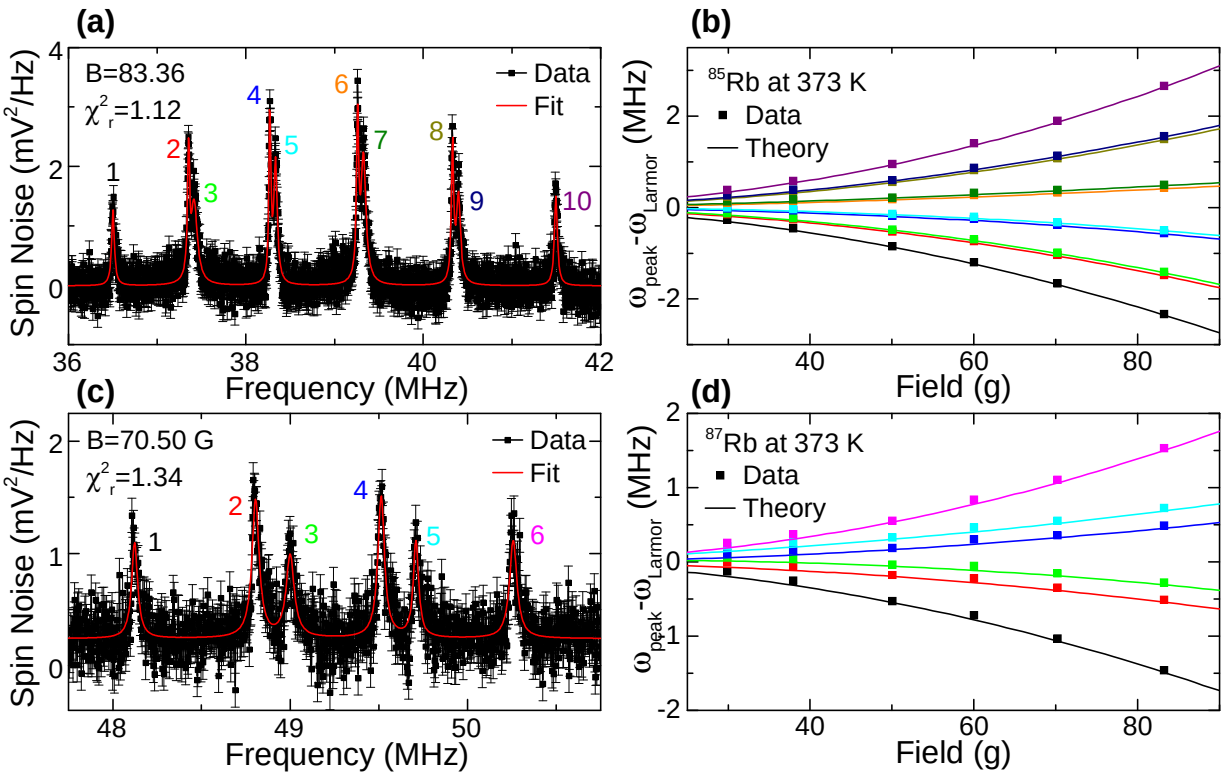

Figure 15: Noise spectra and Zeeman splittings for ^{85}Rb and ^{87}Rb. Data was taken at T=373 K, 25 GHz laser detuning from the D2 transition (780nm) and a power of 1.0 mW. **a,c,** ^{85}Rb and ^{87}Rb splitting, Lorentzian decomposition fits are shown. Error bars are the standard deviation of points in a flat region of the spectrum. **b,d,** Breit–Rabi expected values (solid curves) are shown along with data points for ^{85}Rb and ^{87}Rb. The low field Zeeman energy background given by Eq.1, which scales linearly with applied field, was removed to highlight the quadratic Zeeman and nuclear Zeeman splittings. Error bars are indistinguishable.

References

[1] W. Happer and B. S. Mathur. "Off–resonant light as a probe of optically pumped alkali vapors." *Phys. Rev. Lett.* **18**, 577–580 (1967).

[2] R. Kubo, The "fluctuation-dissipation theorem." *Rep. Prog. Phys.* **29**, 255 (1966).

[3] *Optical Pumping of Rubidium OP1-A Guide to the Experiment* (TeachSpin Inc., 2002).

[4] R. Mansuripur, *Classical Optics and its Applications* (Cambridge University Press, 2009).

[5] S. A. Crooker, D. G. Rickel, A. V. Balatsky, and D. L. Smith. "Spectroscopy of spontaneous spin noise as a probe of spin dynamics and magnetic resonance." *Nature* **431**, 49–52 (2004).

[6] C. H. H. Schule, G. M. Müller, H. Horn, J. Hübner, and M. Oestreich, "Analyzing atomic noise with a consumer sound card," *American Journal of Physics* **80**, 240 (2012).

[7] B. Mihaila, S. A, Crooker, D. G. Rickel, K. Blagoev, P. B. Littlewood, and D. L. Smith. "Quantitative study of spin noise spectroscopy in a classical gas of ^{41}K atoms." *Phys. Rev. A* **74**, 043819 (2006).

[8] E. Arimondo, M. Inguscio, and P. Violino. "Experimental determinations of the hyperfine structure in the alkali atoms." *Rev. Mod. Phys*, **49**(1):33-75, (1977).

[9] S. Bize, Y. Sortais, M. S. Santos, C. Mandache, A. Clairon, and C. Salomon. "High-accuracy measurement of the ^{87}Rb ground-state hyperfine splitting in an atomic fountain," *Europhysics Letters* **45**, 558 (1999).

[10] R. David, *CRC Handbook of Chemistry and Physics*, 82nd ed. (CRC Press, Boca Raton, 2001).

[11] D. Steck, "Alkali D Line Data", **http://steck.us/alkalidata/** (Accessed July, 2014).

[12] "The 2010 CODATA Recommended Values", **http://physics.nist.gov/cuu/Constants/** (Accessed July, 2014).